

Enhancing quantum metrology for multiple frequencies of oscillating magnetic fields by quantum control

Xin Lei(雷昕), Jingyi Fan(范静怡), and Shengshi Pang(庞盛世)

Citation: Chin. Phys. B, 2024, 33 (**6**): 060304. DOI: 10.1088/1674-1056/ad3430
Journal homepage: http://cpb.iphy.ac.cn; http://iopscience.iop.org/cpb

What follows is a list of articles you may be interested in

Holevo bound independent of weight matrices for estimating two parameters of a qubit

Chang Niu(牛畅) and Sixia Yu(郁司夏)
Chin. Phys. B, 2024, 33 (**2**): 020304. DOI: 10.1088/1674-1056/ad117d

Tolerance-enhanced SU(1,1) interferometers using asymmetric gain

Jian-Dong Zhang(张建东) and Shuai Wang(王帅)
Chin. Phys. B, 2023, 32 (**1**): 010306. DOI: 10.1088/1674-1056/ac981d

Improving the teleportation of quantum Fisher information under non-Markovian environment

Yan-Ling Li(李艳玲), Yi-Bo Zeng(曾艺博), Lin Yao(姚林), and Xing Xiao(肖兴)
Chin. Phys. B, 2023, 32 (**1**): 010303. DOI: 10.1088/1674-1056/ac6497

Beating standard quantum limit via two-axis magnetic susceptibility measurement

Zheng-An Wang(王正安), Yi Peng(彭益), Dapeng Yu(俞大鹏), and Heng Fan(范桁)
Chin. Phys. B, 2022, 31 (**4**): 040309. DOI: 10.1088/1674-1056/ac4229

Topological properties of non-Hermitian Creutz ladders

Hui-Qiang Liang(梁辉强) and Linhu Li(李林虎)
Chin. Phys. B, 2022, 31 (**1**): 010310. DOI: 10.1088/1674-1056/ac3991

Enhancing quantum metrology for multiple frequencies of oscillating magnetic fields by quantum control

Xin Lei(雷昕), Jingyi Fan(范静怡), and Shengshi Pang(庞盛世)[†]

School of Physics, Sun Yat-sen University, Guangzhou 510275, *China*

(Received 23 January 2024; revised manuscript received 4 March 2024; accepted manuscript online 15 March 2024)

Quantum multi-parameter estimation has recently attracted increased attention due to its wide applications, with a primary goal of designing high-precision measurement schemes for unknown parameters. While existing research has predominantly concentrated on time-independent Hamiltonians, little has been known about quantum multi-parameter estimation for time-dependent Hamiltonians due to the complexity of quantum dynamics. This work bridges the gap by investigating the precision limit of multi-parameter quantum estimation for a qubit in an oscillating magnetic field model with multiple unknown frequencies. As the well-known quantum Cramér–Rao bound is generally unattainable due to the potential incompatibility between the optimal measurements for different parameters, we use the most informative bound instead which is always attainable and equivalent to the Holevo bound in the asymptotic limit. Moreover, we apply additional Hamiltonian to the system to engineer the dynamics of the qubit. By utilizing the quasi-Newton method, we explore the optimal schemes to attain the highest precision for the unknown frequencies of the magnetic field, including the simultaneous optimization of initial state preparation, the control Hamiltonian and the final measurement. The results indicate that the optimization can yield much higher precisions for the field frequencies than those without the optimizations. Finally, we study the robustness of the optimal control scheme with respect to the fluctuation of the interested frequencies, and the optimized scheme exhibits superior robustness to the scenario without any optimization.

Keywords: quantum metrology, multi-parameter estimation, quantum control

PACS: 03.65.Ta, 03.67.–a **DOI:** 10.1088/1674-1056/ad3430

1. Introduction

Metrology is a subject which explores the methods to enhance measurement precision in various parameter estimation tasks. It plays a pivotal role in scientific research and engineering applications. Metrology is rooted in the classical parameter estimation theory.[1–4] With the advancement in quantum technologies, quantum noise has posed a new challenge to precision measurements. To surpass the classical limit and attain higher precision in physical measurements, quantum technologies are necessary to mitigate the impact of quantum noise on measurement precision. Over the past few decades, quantum metrology has made substantial progress, both theoretically[5–22] and experimentally.[23–38] For instance, researchers have employed quantum error correction techniques[10–15,22] to counteract the effects of quantum noise on measurement precision and used dynamic decoupling[16] to enhance the precision of parameter estimation. Moreover, experiments of quantum metrology have been realized with trapped ions,[27] photon interferometry,[28,36,37] *etc.*,[26,29,38] and applied to quantum imaging,[30–32] biological measurements,[33] and so forth. In addition, researchers have also shown that an entangled ancilla can even overcome the incompatibility completely in multi-parameter quantum estimation.[18,34]

The parameters of interest in quantum metrology are typically associated with the dynamical evolution of quantum systems, such as the intensity of a magnetic field or the relative phase between two arms of an interferometer. In order to obtain the parameters in the quantum dynamics, one needs to encode the parameter into a quantum state by letting a quantum system evolving through the given quantum dynamics, and measure the final states to estimate the parameters. To reach a high precision in estimating the parameters, the parameter estimation theory needs to be invoked. The classical parameter estimation theory is to find an appropriate estimation strategy for a given probability distribution dependent on the unknown parameters, with the goal of achieving the highest precision for the estimate of the parameters. This precision is characterized by the Cramér–Rao bound,[39] where the key statistics is the Fisher information which determines the lower bound of the variance of the parameter estimates. When the unknown parameters are encoded in a quantum system, different measurement bases on the quantum system lead to distinct probability distributions of the measurement outcomes and thus different precisions of parameter estimation, so one needs to identify the optimal measurement bases on the quantum state to achieve the highest precision of parameter estimation.[40,41] This is the primary task of quantum parameter estimation. The maximum Fisher information over all possible quantum measurement bases is referred to as the quan-

[†]Corresponding author. E-mail: pangshsh@mail.sysu.edu.cn

© 2024 Chinese Physical Society and IOP Publishing Ltd

tum Fisher information, and the classical Cramér–Rao bound is generalized to the quantum Cramér–Rao bound for quantum parameter estimation. In quantum metrology, when a quantum system undergoes a dynamical evolution and arrives at a final state containing the unknown parameters, the quantum parameter estimation theory can be applied to design the optimal quantum measurement scheme and the optimal parameter estimation strategy to achieve the highest precision in estimating the parameters.

While the single-parameter quantum estimation theory has been studied extensively, however, in practical quantum metrology problems, there are often multiple unknown parameters to estimate, as encountered in observational astronomy,[42] quantum imaging,[43] quantum sensing,[44] and quantum Hamiltonian identification.[45–48] In classical parameter estimation, the single-parameter Cramér–Rao inequality can be extended to the multi-parameter case, where the variance of the estimates is transformed into a covariance matrix between different parameters, and the Fisher information becomes the Fisher information matrix.[49] A notable characteristic of the classical multi-parameter estimation is that the Cramér–Rao bound can always be asymptotically achieved as the sample size tends to be infinite. In contrast, the quantum multi-parameter estimation is more intricate. For quantum multi-parameter estimation, the single-parameter quantum Cramér–Rao inequality can be extended to the multi-parameter case with a lower bound determined by the quantum Fisher information matrix. Helstrom[50] and Yuen and Lax,[51] in parallel with Belavkin,[52] proposed the most renowned and useful methods to define the quantum Fisher information matrix based on the symmetric logarithmic derivatives (SLD), which lead to the SLD-Cramér–Rao bound. But unlike the classical multi-parameter estimation, the optimal measurements for different parameters in quantum multi-parameter estimation are not necessarily compatible between each other, implying that the optimal precisions for different parameters may not be simultaneously achievable. To achieve the highest estimation precisions for all parameters simultaneously in quantum multi-parameter estimation, the quantum state to be measured needs to meet strict conditions. Currently, only a few number of quantum models are known to satisfy the conditions for simultaneously optimizing the precision for multiple parameters: according to Suzuki's classification in Ref. [53], the SLD-Cramér–Rao bound can be achieved only in the classical quantum statistical models,[54] the quasi-classical quantum statistical models,[55] and asymptotically saturated in the asymptotically classical quantum statistical models.[55] Therefore, in more general cases, the SLD-Cramér–Rao bound cannot be achieved generally, which is why the quantum multi-parameter estimation is a challenging problem.

A pivotal task in quantum metrology is to design measurement schemes that achieve the highest precision for unknown parameters. Since the unknown parameters of interest are often related to quantum dynamics, and quantum measurements target quantum states, it is necessary to encode unknown parameters into appropriate quantum states. The processes of parameter estimation can be generally divided into four steps (see the standard scheme in Fig. 1): the preparation of the quantum system in a specific initial state, the evolution of the quantum system under the given dynamics dependent on the unknown parameters, the measurement on the final state of the system and the estimation of the unknown parameters from the measurement results.[41] As the final state of the quantum system's evolution determines the precision of parameter measurement, it is essential for the quantum system to evolve to a final state that contains as much parameter information as possible. There are various methods to optimize the final state of the quantum system, e.g., assuming the dynamical evolution fixed and enhancing the measurement precision by preparing an optimized initial state,[6,56–65] introducing a Hamiltonian control that is independent of parameters to optimize the evolution path of the quantum system to acquire the most information about the parameters (see the controlled scheme in Fig. 1),[7,8,17,18,66] etc. Moreover, in recent years, researchers have found that the additional controls on the quantum evolution can not only provide a higher precision limit, but also brings greater robustness to the estimation processes.[9,35,67]

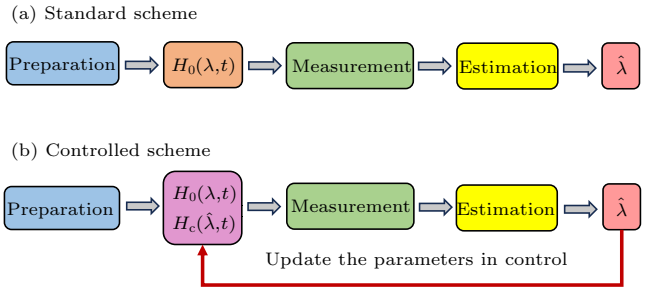


Fig. 1. General processes of quantum metrology: (a) standard scheme and (b) controlled scheme. In panel (a), a probe state evolves under the encoding Hamiltonian $H_0(\boldsymbol{\lambda},t)$ with the unknown parameter $\boldsymbol{\lambda}$. Proper measurements are then performed on the final state to extract the information of the parameter $\boldsymbol{\lambda}$. (b) In panel (b), the system starts from an initial probe state. The encoding dynamics is engineered with an adaptive Hamiltonian control $H_c(\hat{\boldsymbol{\lambda}},t)$, where $\hat{\boldsymbol{\lambda}}$ is an approximate value of $\boldsymbol{\lambda}$. The final state is then measured to estimate the unknown parameters, and the control parameters are iteratively updated by the results from the previous iterations.

While the most of existing researches on the quantum multi-parameter estimation have focused on measuring parameters in time-independent Hamiltonians,[7,18] the investigation of the multi-parameter quantum estimation for systems with time-dependent Hamiltonians remains limited due to the complexity of the quantum dynamics in this case. In the present study, we bridge this gap by investigating the precision limit of the multi-parameter quantum estimation for

a qubit evolving in an oscillating magnetic fields with multiple unknown parameters. Since the well-known quantum SLD-Cramér–Rao bound is generally unachievable, we introduce the most informative bound[54] to quantify the precision limit of the multi-parameter quantum estimation by optimizing the classical multi-parameter Cramér–Rao bound over all possible measurement bases on the quantum system. Note that this bound is different from the quantum Cramér–Rao bound: while the single-parameter quantum Cramér–Rao bound is the optimization of the classical single-parameter Cramér–Rao bound over all quantum measurement bases, the multi-parameter quantum Cramér–Rao bound is not the optimization of the multi-parameter classical Cramér–Rao bound but rather just a mathematical generalization of the single-parameter quantum Cramér–Rao bound by straightforwardly extending the single-parameter quantum Fisher information to multi-parameter quantum Fisher information matrix.

Motivated by the aforementioned optimization approaches, we simultaneously employ the optimization of initial state preparation, Hamiltonian control and final measurements to achieve the highest estimation precision. Numerical optimization algorithms include the gradient ascent pulse engineering (GRAPE),[68] Newton's and the quasi-Newton method,[69] etc. Due to the slow convergence of the GRAPE algorithm and the computational burden of Newton's method involving the computation of second-order derivatives, we employ the quasi-Newton method in this work, which accelerates the speed of convergence by constructing a matrix approximately equal to the Hessian matrix but using only the first-order derivatives. Through the quasi-Newton method, we investigate the optimal scheme involving the optimal initial state preparation, the optimal controls and the optimal measurements to enhance the precision of estimating the multiple unknown frequencies by measuring the qubit evolving in the oscillating magnetic field. It should be noted that, as the quasi-Newton method is essentially a gradient-based method, the optimization here refers to local optimization similar to other literatures.[7,8] Additionally, we also explore the robustness of the optimized scheme against the fluctuations of the parameters in the Hamiltonian, and study the trade-off between the estimation precisions of different parameters in this problem.

The paper is organized as follows. In Section 2, we introduce the general theory of multi-parameter quantum estimation and the definition of the most informative bound. Section 3 is devoted to introducing the model of a qubit interacting with an oscillating magnetic field with multiple unknown frequencies and deriving the most informative bound, as well as corresponding gradient functions. Detailed analysis of results are given in Section 4, including optimal multi-parameter estimation, robustness, and trade-off. Finally the paper is concluded in Section 5.

2. Preliminaries

In this section, we briefly introduce the fundamental concepts of parameter estimation theory and the most informative bound.

2.1. Multi-parameter quantum estimation

Generally, to estimate multiple parameters $\boldsymbol{\lambda} = (\lambda_1, \lambda_2, \lambda_3, \ldots, \lambda_d)$, one should encode them in a quantum state $\rho_{\boldsymbol{\lambda}}$, then performs a quantum measurement described by positive operator-valued measure (POVM), $\Pi = \{\Pi_k\}$, where $\Pi_k \geq 0$ and $\sum_k \Pi_k = \mathbb{I}$. According to the Born rule, the probability to observe the k-th result is given by $p(k|\boldsymbol{\lambda}) = \mathrm{Tr}[\rho_{\boldsymbol{\lambda}}\Pi_k]$. The parameters are estimated through an estimator $\hat{\boldsymbol{\lambda}} = (\hat{\lambda_1}, \hat{\lambda_2}, \hat{\lambda_3}, \ldots, \hat{\lambda_d})$, which is a map from the measurement outcomes to the possible values of the parameters. The precision of the estimation is typically quantified by the covariance matrix C with the entries

$$C_{\alpha\beta} = \sum_k p(k|\boldsymbol{\lambda})(\hat{\lambda_\alpha} - \lambda_\alpha)(\hat{\lambda_\beta} - \lambda_\beta). \tag{1}$$

It can be seen that the diagonal entries of the covariance matrix are the variances for the corresponding parameters, thereby $\mathrm{Tr}[C]$ represents the sum of variances for each parameter, making it suitable for quantifying the overall precision of multi-parameter estimation. The classical Cramér–Rao inequality,[2,70]

$$C \geq F^{-1}, \tag{2}$$

imposes a constraint on the covariance matrices over all possible estimation strategies in terms the classical Fisher information matrix (CFIM) with elements

$$F_{\alpha\beta} = \sum_k p(k|\boldsymbol{\lambda})(\partial_{\lambda_\alpha} \log p(k|\boldsymbol{\lambda}))(\partial_{\lambda_\beta} \log p(k|\boldsymbol{\lambda})). \tag{3}$$

Hence, to achieve a high estimation precision, it is necessary to minimize the classical Cramér–Rao bound.

When the classical Cramér–Rao bound is applied to the quantum parameter estimation, different measurement bases on the quantum system leads to different probability distributions of the measurement results, and thus will have different Cramér–Rao bounds. The quantum parameter theory tells that for all possible measurement bases, the following inequality always stands true for the covariance matrix C and is determined by the quantum statistical model only,

$$C \geq Q^{-1}, \tag{4}$$

where Q is the quantum Fisher information matrix. This inequality is called the quantum Cramér–Rao bound.

There are different approaches to the derivation of the quantum Fisher information matrix. The most celebrated ones have been pursued by Helstrom[50] and Yuen and Lax[51] (in parallel to Belavkin[52]) by introducing the symmetric logarithmic derivative (SLD) operators L_α^S defined by $\partial_{\lambda_\alpha}\rho_{\boldsymbol{\lambda}} = (L_\alpha^S\rho_{\boldsymbol{\lambda}} + \rho_{\boldsymbol{\lambda}}L_\alpha^S)/2$. And the quantum Fisher information matrix is defined with elements

$$Q_{\alpha\beta}^S = \mathrm{Tr}\left[\rho_{\boldsymbol{\lambda}}\frac{L_\alpha^S L_\beta^S + L_\beta^S L_\alpha^S}{2}\right]. \tag{5}$$

The quantum Cramér–Rao bound by plugging Eq. (5) into Eq. (4) is usually called SLD Cramér–Rao bound.

Unlike the classical Cramér–Rao bound, the quantum Cramér–Rao bound is not always attainable, for which the intuitive reason is the potential incompatibility between the optimal measurements for different parameters. According to the classification by Suzuki,[53] the following are the major types of quantum states that can satisfy the conditions of simultaneous optimization for the precisions of all parameters: (i) Classical quantum statistical models: the density matrix $\rho_{\boldsymbol{\lambda}}$ can be diagonalized by a λ-independent unitary transformation, $\rho_{\boldsymbol{\lambda}} = U\Lambda_{\boldsymbol{\lambda}}U^\dagger$, where $\Lambda_{\boldsymbol{\lambda}}$ is a diagonal matrix, then the SLD Cramér–Rao bound is attainable, by taking the eigenbasis of $\rho_{\boldsymbol{\lambda}}$ as the measurement bases for all the parameters;[54] (ii) Quasi-classical quantum statistical models: all SLD operators commute with each other, $[L_\alpha^S, L_\beta^S] = 0$, then the SLD Cramér–Rao bound is also attainable because there is a single eigenbasis for all the SLD operators;[55] (iii) Asymptotically classical quantum statistical models: all the SLD operators commute on average over $\rho_{\boldsymbol{\lambda}}$, $\mathrm{Tr}[\rho_{\boldsymbol{\lambda}}L_\alpha^S L_\beta^S] = 0$, then the SLD Cramér–Rao bound can be saturated asymptotically by a collective measurement on an asymptotically large number of copies $\rho_{\boldsymbol{\lambda}}^{\otimes n}$, in which case the SLD Cramér–Rao bound is equivalent to the well-known Holevo bound.[55]

2.2. Most informative bound

As the quantum Cramér–Rao bound is not saturable except for special types of quantum states as reviewed above, we introduce the most informative bound[54] to evaluate the precision of multi-parameter quantum estimation in this work, a minimization of the classical multi-parameter Cramér–Rao bound over all possible POVM's,

$$F_{\mathrm{MI}} = \min_{\{M_i\}} \mathrm{Tr}F^{-1}, \tag{6}$$

where $\{M_i\}$ is an arbitrary set of POVM elements, and F_{MI} denotes the mean precision limit of all parameters. As the considered system is an isolated qubit system, the most informative bound can be written as

$$F_{\mathrm{MI}} = \min_{M_1,M_2} \mathrm{Tr}F^{-1}, \tag{7}$$

where M_1, M_2 represent a pair of possible orthogonal projective operators on the qubit. It is obvious that the most informative bound is always attainable by definition, and in fact, it is also equivalent to the Holevo bound in the asymptotic limit.

3. Model of qubit in an oscillating magnetic field

Most of the previous researches on quantum multi-parameter estimation have focused on quantum systems with time-independent Hamiltonians. In this work, we consider a qubit system in an oscillating magnetic field with multiple unknown frequencies as an example to study the multi-parameter quantum metrology with time-dependent Hamiltonians.

3.1. Hamiltonian and unitary evolution

The Hamiltonian of the current model can be written as

$$H(t) = H_0(t) + H_{\mathrm{c}}(t), \tag{8}$$

where

$$H_0(t) = -B(\cos\omega_1 t\sigma_1 + \sin\omega_2 t\sigma_3), \tag{9}$$

σ_1 and σ_3 are Pauli matrices, and ω_1 and ω_2 are the unknown frequencies to be estimated. For a controlled scheme, controls are applied on the Hamiltonian of the qubit, which can be generally written as

$$H_{\mathrm{c}}(t) = \sum_{i=1}^{3} V_i(t)\sigma_i. \tag{10}$$

The initial state of the probe is assumed to be

$$|\psi(0)\rangle = \cos\theta_0|0\rangle + \mathrm{e}^{\mathrm{i}\varphi_0}\sin\theta_0|1\rangle. \tag{11}$$

For the simplicity of notation, we denote the two unknown frequencies ω_1 and ω_2 as a vector, $\boldsymbol{\omega} = (\omega_1, \omega_2)$.

After a unitary evolution of time t under the Hamiltonian $H(t)$ [Eq. (8)], the state of the qubit becomes

$$|\psi_{\boldsymbol{\omega}}(t)\rangle = U_{\boldsymbol{\omega}}(0\to t)|\psi(0)\rangle, \tag{12}$$

where $U_{\boldsymbol{\omega}}(0\to t)$ is the unitary evolution operator dependent on the frequencies ω_1 and ω_2,

$$U_{\boldsymbol{\omega}}(0\to t) = \mathcal{T}\,\mathrm{e}^{-\mathrm{i}\int_0^t H(\tau)\,\mathrm{d}\tau}, \tag{13}$$

and $\mathcal{T}$ denotes the time-ordering operator.

3.2. Most informative bound

The orthogonal projective measurement operators on the final state of the qubit after the unitary evolution can be written as

$$M_1 = |m_1\rangle\langle m_1|, \quad M_2 = |m_2\rangle\langle m_2|, \tag{14}$$

where

$$|m_1\rangle = \cos\theta_1|0\rangle + \mathrm{e}^{\mathrm{i}\varphi_1}\sin\theta_1|1\rangle, \tag{15}$$

$$|m_2\rangle = \mathrm{e}^{-\mathrm{i}\varphi_1}\sin\theta_1|0\rangle - \cos\theta_1|1\rangle. \tag{16}$$

The probability to obtain the k-th result, $k = 1, 2$, is given by

$$p_{\omega}^{(k)}(t) = |\langle m_k|\psi_{\omega}(t)\rangle|^2. \tag{17}$$

In order to quantify the precision of estimating the unknown frequencies, we invoke the well-known Cramér–Rao bound from the classical parameter estimation theory, which was reviewed in Subsection 2.1. The elements of Fisher information matrix can be obtained by Eq. (3) as

$$\begin{aligned} F_{\alpha\beta}(t) &= \sum_{k=1}^{2} p_{\omega}^{(k)}(t)(\partial_{\omega_\alpha}\log p_{\omega}^{(k)}(t))(\partial_{\omega_\beta}\log p_{\omega}^{(k)}(t)) \\ &= \sum_{k=1}^{2}\frac{\langle m_k|\partial_{\omega_\alpha}\rho_{\omega}(t)|m_k\rangle\langle m_k|\partial_{\omega_\beta}\rho_{\omega}(t)|m_k\rangle}{\langle m_k|\rho_{\omega}(t)|m_k\rangle}, \end{aligned} \tag{18}$$

where

$$\begin{aligned} &\partial_{\omega_i}\rho_{\omega}(t) = |\partial_{\omega_i}\psi_{\omega}(t)\rangle\langle\psi_{\omega}(t)| + |\psi_{\omega}(t)\rangle\langle\partial_{\omega_i}\psi_{\omega}(t)|, \\ &i = 1, 2, \end{aligned} \tag{19}$$

and the Cramér–Rao bound is given by Eq. (2). As the dependence of $|\psi_{\omega}(t)\rangle$ on the frequencies ω_1, ω_2 stems from the unitary evolution $U_{\omega}(0\to t)$ [Eq. (13)] in which ω_1 and ω_2 have been encoded, the derivatives of $|\psi_{\omega}(t)\rangle$ with respect to ω_1 and ω_2 can be written as

$$|\partial_{\omega_i}\psi_{\omega}(t)\rangle = [\partial_{\omega_i}U_{\omega}(0\to t)]|\psi(0)\rangle. \tag{20}$$

To quantify the overall precision of estimating different parameters, we take the trace of the Cramér–Rao bound to give a uniformly-weighted average of the precisions for different parameters. If we further minimize the trace of Cramér–Rao bound over all possible measurement bases, we can obtain the most informative bound

$$\begin{aligned} F_{\mathrm{MI}}(t) &= \min_{M_1,M_2}\mathrm{Tr}[F^{-1}(t)] \\ &= \min_{M_1,M_2}\frac{F_{11}(t)+F_{22}(t)}{(F_{11}(t)F_{22}(t)-F_{12}(t)^2)}. \end{aligned} \tag{21}$$

3.3. Derivatives for quasi-Newton method

In order to enhance the sensitivity of estimating the unknown frequencies of the magnetic field, it is necessary to optimize the initial state of the qubit, the Hamiltonian control and the final measurement on the qubit, i.e., to find the optimal set of parameters $\{\theta_0, \varphi_0, \theta_1, \varphi_1, V_1(\tau), V_2(\tau), V_3(\tau)\}$, $0 \le \tau \le t$, to minimize the most informative bound $F_{\mathrm{MI}}(t)$. It can be seen from Eq. (21) that the most informative bound $F_{\mathrm{MI}}(t)$ is so complex that it can be hardly minimized by any analytical approach, so we take a numerical method to carry out the optimization.

As reviewed in Appendix A, the quasi-Newton method has the advantage of fast convergence speed compared to the steepest descent method and low computational complexity compared to the Newton's method, so we take the quasi-Newton method to optimize the most informative bound in this work. The crucial step of the quasi-Newton method is to calculate the gradient of the objective function with respect to the parameters to be optimized. So, we show how to obtain the gradient of the most informative bound below.

The derivatives of the most informative bound with respect to the parameters in the initial state and the measurement basis can be straightforwardly attributed to the derivatives of the initial state and the measurement basis, so we omit the detail here. The difficulty of deriving the gradient of the most informative bound lies in the computation of the first-order and second-order derivatives of the final state with respect to the parameters $\{\omega_1, \omega_2, V_1(\tau), V_2(\tau), V_3(\tau)\}$. As these parameters are all related to the evolution of the qubit and have been encoded in the unitary evolution operator $U_{\omega}(0\to t)$ [Eq. (13)], the derivatives of the final state with respect to these parameters can be boiled down to the derivatives of $U_{\omega}(0\to t)$. Below we show how to compute the derivatives of $U_{\omega}(0\to t)$ with respect to these parameters.

For simplicity, we denote the i-th parameter from the set $\{\omega_1, \omega_2, V_1(\tau), V_2(\tau), V_3(\tau)\}$ as g_i. The first-order derivative of $U_{\omega}(0\to t)$ with respect to g_i can be shown as

$$\begin{aligned} &\partial_{g_i}U_{\omega}(0\to t) \\ &= -\mathrm{i}\int_0^t U_{\omega}(\tau\to t)\partial_{g_i}H(\tau)U_{\omega}(0\to\tau)\,\mathrm{d}\tau, \end{aligned} \tag{22}$$

by dividing $U_{\omega}(0\to t)$ into minor unitary evolutions of infinitely many short time intervals and taking the derivative of the minor unitary evolution in each short time interval. The second-order derivative of $U_{\omega}(0\to t)$ with respect to g_i and g_j can be similarly shown as

$$\begin{aligned} &\partial_{g_i}\partial_{g_j}U_{\omega}(0\to t) \\ &= -\int_{\tau_2}^{t}\int_{\tau_1}^{\tau_2} U_{\omega}(\tau_2\to t)\partial_{g_j}H(\tau_2)U_{\omega}(\tau_1\to\tau_2) \end{aligned}$$

$$\times\partial_{g_i}H(\tau_1)U_{\boldsymbol{\omega}}(0\to\tau_1)\,\mathrm{d}\,\tau_1\,\mathrm{d}\,\tau_2$$
$$-\int_{\tau_2}^{t}\int_{\tau_1}^{\tau_2}U_{\boldsymbol{\omega}}(\tau_2\to t)\partial_{g_i}H(\tau_2)U_{\boldsymbol{\omega}}(\tau_1\to\tau_2)$$
$$\times\partial_{g_j}H(\tau_1)U_{\boldsymbol{\omega}}(0\to\tau_1)\,\mathrm{d}\,\tau_1\,\mathrm{d}\,\tau_2$$
$$-\mathrm{i}\int_0^t U_{\boldsymbol{\omega}}(\tau\to t)\partial_{g_i}\partial_{g_j}H(\tau)U_{\boldsymbol{\omega}}(0\to\tau)\,\mathrm{d}\,\tau. \quad (23)$$

Once the derivatives of $U_{\boldsymbol{\omega}}(0\to t)$ as well as the derivatives of probe state and measurement basis with respect to these parameters are obtained, the gradient of the most informative bound F_{MI} [Eq. (21)] can be derived, and the gradient can be then applied in the iterations of the quasi-Newton algorithm to find the optimal parameters $\{\theta_0,\varphi_0,\theta_1,\varphi_1,V_1(\tau),V_2(\tau),V_3(\tau)\}$ that minimize the most informative bound F_{MI}.

4. Optimization results and discussion

4.1. Optimal multi-parameter estimation

Firstly, we consider the case without any optimization on the initial state or the Hamiltonian control. We compare the classical Cramér–Rao bound with the most informative bound under free evolution. It can be seen from Fig. 2 that the most informative bound is tighter than the classical Cramér–Rao bound, so the most informative bound can provide a more exact quantification of the highest precision that the multi-parameter estimation of the unknown frequencies can achieve in the current model. It should be noted that according to the definition of the most informative bound, the most informative bound obtained without any optimization can actually still outperform the classical Cramér–Rao bound due to the optimization of the measurement basis.

Then, we turn to the scenario that only the initial state is optimized by the quasi-Newton method. Figure 3 shows that the precision of the scheme without any optimization (solid blue line in Fig. 3) and that only with optimal initial state (solid orange line in Fig. 3) are fairly close, but the precision of the latter one performs better at certain time moments, which indicates that the optimal initial state can contribute slight increase in the precision limit of estimating the unknown frequencies. Now if we further employ the optimal control on the Hamiltonian obtained via the quasi-Newton method, the most informative bound can be improved significantly, which is shown in Fig. 3. This indicates that the controls on the Hamiltonian are more capable of enhancing the precision limit than that on the initial state. It should be noted that for the sake of numerical calculation, we divide the time-continuous controls into piecewise controls. In the figure, the controls over the time interval from 0 to the target time t are divided into 50 pieces.

Figure 4 compares the most informative bound with the SLD Cramér–Rao bound. It can be seen that the SLD Cramér–Rao bound is not as tight as the most informative bound, which implies the SLD Cramér–Rao bound is an over-optimistic bound for the estimation precision of the unknown frequencies and shows the superiority of the most informative bound in quantifying the precision limit of quantum multi-parameter estimation.

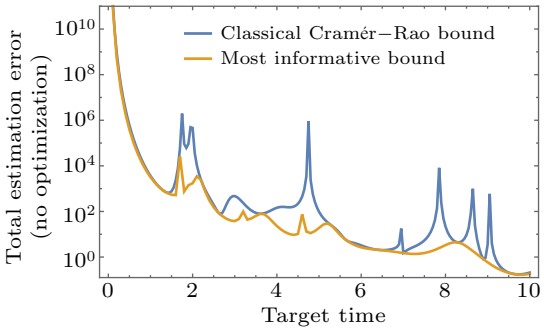


Fig. 2. Comparison between the classical Cramér–Rao bound (the solid blue line) and the most informative bound (the solid orange line) without any optimization as functions of the target time t. The true values for B, ω_1, and ω_2 are 1.2, 1, and 1.1, and the initial state $|\psi_0\rangle$ is $|0\rangle$. It can be observed that the most informative bound is tighter than the classical Cramér–Rao bound for the precision limit that the multi-parameter estimation can achieve.

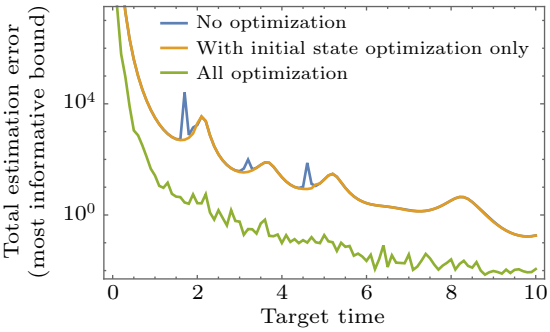


Fig. 3. The most informative bound as a function of the target time t. The solid blue line and the orange line represent the scheme without any optimization and that only with the initial state optimized respectively, while the solid green line denotes the scheme with both optimizations of the initial state and the Hamiltonian control. It can be observed that the most informative bound outperforms the classical Cramér–Rao bound, as it implicitly includes the optimization of the measurement on the final state by its definition. The true values for B, ω_1, and ω_2 are 1.2, 1, and 1.1. It can be seen that the scheme with all optimizations can increase the precision by several orders of magnitude.

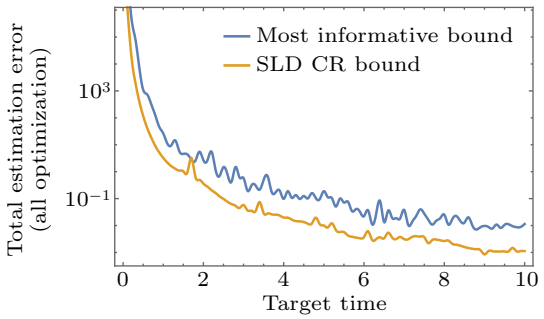


Fig. 4. Comparison between the most informative bound (the solid blue line) and the SLD CR bound (the solid orange line), both with all optimizations, as functions of the target time t. The true values for B, ω_1, and ω_2 are 1.2, 1, and 1.1. It can be observed that the SLD Cramér–Rao bound is an over-optimistic bound and not always attainable, so the most informative bound can describe the precision limit of multi-parameter estimation more exactly.

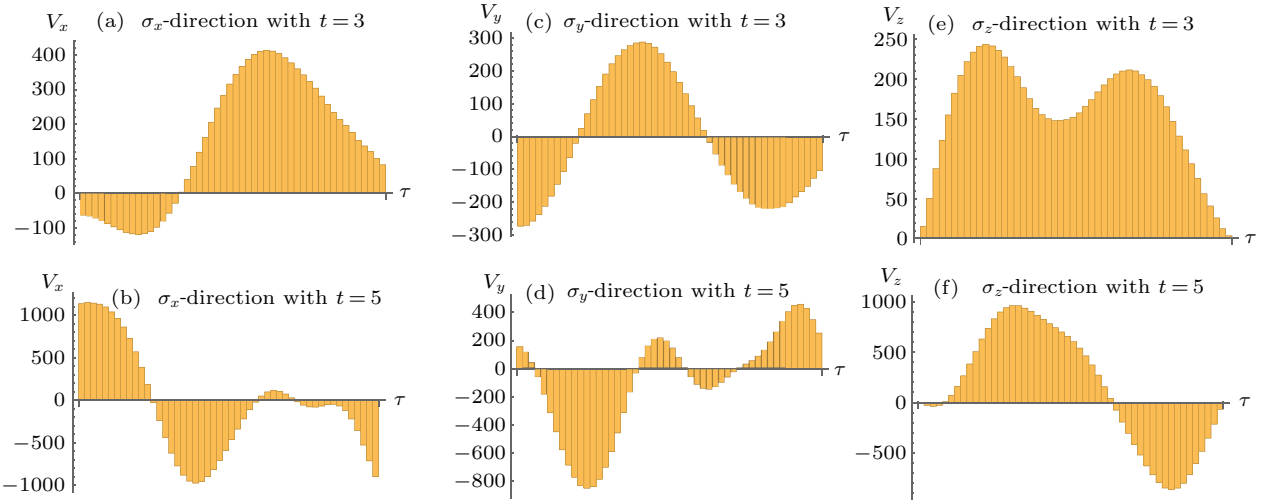


Fig. 5. Optimal controls on the σ_x, σ_y, σ_z components of the Hamiltonian obtained by the quasi-Newton method over the time intervals from 0 to the target time $t=3$ and $t=5$.

It is worth noting that the optimal initial state and optimal Hamiltonian controls are dependent on the target evolution time. When the target evolution time changes, the optimal controls on the initial state and the Hamiltonian vary as well. Figure 5 displays the optimal controls over the time interval from 0 to the target time $t=3$ and $t=5$.

4.2. Robustness

The precision limit of the unknown frequencies as well as the optimal controls on the initial state, the Hamiltonian and the final measurement obtained in the above calculations are generally dependent on the unknown frequencies ω_1 and ω_2. But the unknown frequencies are the parameters to estimate, so we can only use the estimates of these parameters which are usually not the true values of the parameters. Due to the discrepancies between the estimated values and the true values of the frequencies, the real precision limit may differ from the theoretical precision limit obtained by applying the true values of the parameters in the optimal controls. So, it is important to investigate how the precision limit may decrease due to this discrepancy.

In this subsection, we study the robustness of the optimized quantum metrology scheme against the deviations between the approximate values of the frequencies used in deriving the optimal controls and the true values of the frequencies. If the precision limit of estimating the frequencies does not decrease significantly when the true values of the parameters lie within a vicinity of the approximate parameter values, the optimized quantum metrology scheme can be deemed robust. In order to characterize the robustness of the optimized quantum metrology scheme obtained from the above quasi-Newton method, we plot the range of estimation precision limit of the frequencies in response to the deviation of the frequencies at different target moments.

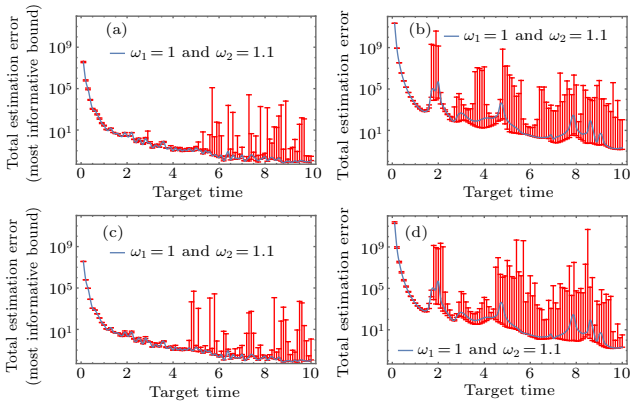


Fig. 6. The precision limit as a function of the target time t within a vicinity of ω_1 or ω_2 around ω_{10} or ω_{20}. (a) Scheme with all optimizations. The red bars represent the ranges of the most informative bound when ω_1 varies from 0.9 to 1.1 and ω_2 is fixed at ω_{20}. (b) Scheme without any optimization. The red bars represent the ranges of total estimation error $\mathrm{Tr}[F^{-1}]$ when ω_1 varies from 0.9 to 1.1 and ω_2 is fixed at ω_{20}. (c) Scheme with all optimizations. The red bars represent the ranges of the most informative bound when ω_2 varies from 1.0 to 1.2 and ω_1 is fixed at ω_{10}. (d) Scheme without any optimization. The red bars represent the ranges of $\mathrm{Tr}[F^{-1}]$ when ω_2 varies from 1.0 to 1.2 and ω_1 is fixed at ω_{10}. The true values for B, ω_1, and ω_2 are 1.2, 1, and 1.1. It can be seen that the optimizations can not only increase the precision by several orders of magnitude but also improve the robustness of the estimation against the deviation between the approximate values of the parameters used in the optimal controls and the true values of the parameters.

Figures 6(a) and 6(c) show the cases with all the optimizations on the initial state, the Hamiltonian and the final measurement basis. The solid blue line denotes the most informative bound with $\omega_1=\omega_{10}$ and $\omega_2=\omega_{20}$ at every target moment, where ω_{10} and ω_{20} are the estimated values of the unknown frequencies. Applying the same optimization scheme to other cases in which the values of ω_1 or ω_2 vary, the range of the most informative bound at every target moment can be obtained. The red bars represent the range of the estimation precision limit at different target moments when ω_1 varies within a range of 10% around ω_{10} or ω_2 varies within a range of 9% around ω_{20}. Estimation results without any optimization are shown in Figs. 6(b) and 6(d). Similar to the case

with optimizations, the solid blue line denotes the most informative bound with $\omega_1 = \omega_{10}$ and $\omega_2 = \omega_{20}$ at every target moment, and the red bars represent the range of estimation precision limit at different target moments when ω_1 or ω_2 varies. It can be concluded by the comparison between these figures that optimization can not only improve the precision limit of estimating the frequencies, but also enhance the robustness of the precision limit against the parameter deviations.

In addition, we plot the contours for the function of $\mathrm{Tr}[F^{-1}]$ versus both ω_1 and ω_2, so as to display the impact of simultaneous variation of ω_1 and ω_2 on the precision limit of estimating the frequencies in Fig. 7. The spacing between the adjacent contour lines in the two subfigures are chosen to be equal so that the two subfigures are comparable. It can be seen that the lines in Fig. 7(b) are denser than those in Fig. 7(a), so the quantum metrology scheme with all optimizations exhibits better robustness than that without any optimization.

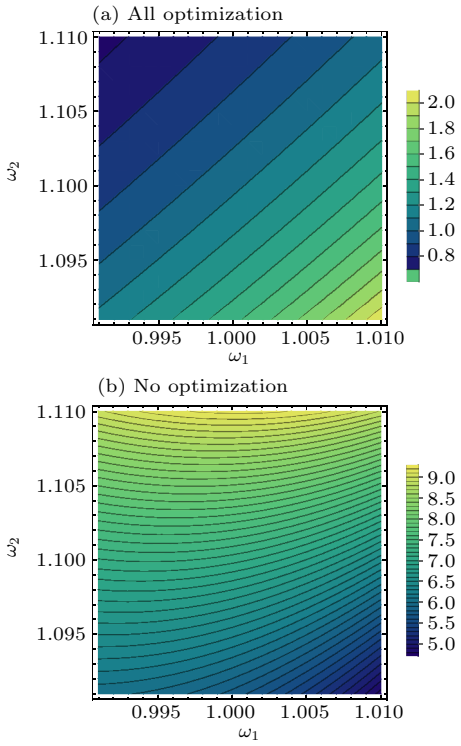


Fig. 7. Contour plots for the total estimation error of the two frequencies as functions of both ω_1 and ω_2 at target time $t = 7.5$, with all the optimizations or without any optimization. The color represents the magnitude of the total estimation error. The true values for B, ω_1, and ω_2 are 1.2, 1, and 1.1.

4.3. Trade-off

In the above sections, we have considered the most informative bound of estimating multiple frequencies with equal weights on the unknown frequencies. In some scenarios, one may be interested in just one or a few of those unknown parameters, so the unknown parameters can be assigned with unequal weights in the sum of the estimation precisions of different parameters. This is actually the quantum estimation with nuisance parameters.[71,72] In this case, the most informative bound can be generalized as

$$F_{\mathrm{MI}}(t) = \min_{M_1,M_2} \mathrm{Tr}[WF^{-1}(t)], \tag{24}$$

where W denotes an arbitrary weight matrix which is usually positive semi-definite and the dependence of the Fisher information matrix F and the related most informative bound F_{MI} on the target time t is explicitly shown. In detail, if equal weights are assigned to both parameters, the weight matrix can be written as $W_{11} = \begin{pmatrix} 1 & 0 \\ 0 & 1 \end{pmatrix}$, which is the case considered above; if the estimation is focused on a single parameter, the weight matrix can be chosen as $W_{10} = \begin{pmatrix} 1 & 0 \\ 0 & 0 \end{pmatrix}$ or $W_{01} = \begin{pmatrix} 0 & 0 \\ 0 & 1 \end{pmatrix}$, corresponding to the estimation of the first parameter or the second parameter respectively.

For the case of equal weights on the two unknown parameters, the most informative bound has been given by Eq. (21).

If the focus is only on the oscillation frequency of the magnetic field along the x direction, i.e., ω_1, the most informative bound can be written as

$$\begin{aligned} F_{\mathrm{MI},\omega_1}(t) &= \min_{M_1,M_2} \mathrm{Tr}[W_{10}F^{-1}(t)] \\ &= \min_{M_1,M_2} \frac{F_{22}(t)}{-F_{12}(t)^2 + F_{11}(t)F_{22}(t)}. \end{aligned} \tag{25}$$

Similarly, if the focus is only on the oscillation frequency of the magnetic field along the z direction, i.e., ω_2, the most informative bound can be written as

$$\begin{aligned} F_{\mathrm{MI},\omega_2}(t) &= \min_{M_1,M_2} \mathrm{Tr}[W_{01}F^{-1}(t)] \\ &= \min_{M_1,M_2} \frac{F_{11}(t)}{-F_{12}(t)^2 + F_{11}(t)F_{22}(t)}. \end{aligned} \tag{26}$$

Moreover, if one of the frequencies is somehow known and the other frequency remains unknown, we just need to measure and estimate the unknown frequency. This becomes a single-parameter estimation problem, and the most informative bound for the two frequencies can be written as

$$F_{\mathrm{single1}}(t) = \min_{M_1,M_2} \frac{1}{F_{11}(t)}, \tag{27}$$

$$F_{\mathrm{single2}}(t) = \min_{M_1,M_2} \frac{1}{F_{22}(t)}. \tag{28}$$

Similar to the approach before, the quasi-Newton method can be exploited to minimize $F_{\mathrm{MI},\omega_1}(t)$, $F_{\mathrm{MI},\omega_2}(t)$, $F_{\mathrm{single1}}(t)$, and $F_{\mathrm{single2}}(t)$, by optimizing the initial state, controls, and measurements. Let

$$F_{\mathrm{m1}}(t) = F_{\mathrm{MI}}^{(\mathrm{opt})}(t), \tag{29}$$

$$F_{\mathrm{m2}}(t) = F_{\mathrm{MI},\omega_1}^{(\mathrm{opt})}(t) + F_{\mathrm{MI},\omega_2}^{(\mathrm{opt})}(t), \tag{30}$$

$$F_{\mathrm{s}}(t) = F_{\mathrm{single1}}^{(\mathrm{opt})}(t) + F_{\mathrm{single2}}^{(\mathrm{opt})}(t), \tag{31}$$

where the superscript (opt) denotes the optimization by the quasi-Newton method. It can be expected that $F_{\mathrm{m1}}(t)$ stands

for the highest precision of simultaneously estimating both frequencies with equal weights in the average, while $F_{\mathrm{m2}}(t)$ denotes the sum of the precisions of simultaneously estimating both frequencies but focusing on only one of the frequencies. $F_{\mathrm{s}}(t)$ represents the sum of the precisions of estimating one of the frequencies assuming the other frequency is known. Figure 8 indicates that even with all the optimizations, the errors of the two multi-parameter estimation schemes, with both frequencies unknown and equally or unequally weighted, are always higher than that of the single-parameter estimation scheme with one of the frequencies assumed to be known. This discrepancy is a manifestation of the difference between multi-parameter and single-parameter quantum estimations, due to the potential incompatibility[25] between the optimal measurements for different parameters and thereby the trade-off of the precisions between different parameters when all the unknown parameters are estimated simultaneously in the quantum multi-parameter estimation.

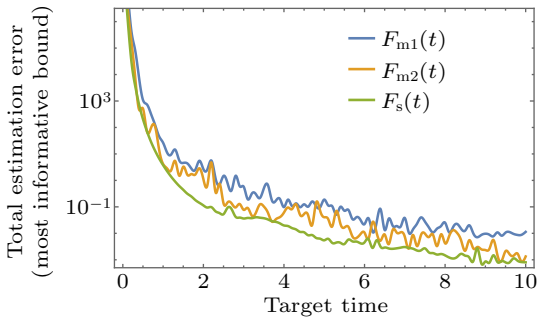


Fig. 8. The most informative bound as a function of the target time t. The solid blue line denotes the lowest total estimation error when the two frequencies are unknown estimated simultaneously, i.e., the weight matrix is $W = \begin{pmatrix} 1 & 0 \\ 0 & 1 \end{pmatrix}$. The orange line represents total estimation error when the two frequencies are both unknown and estimated simultaneously but focusing on one parameter each time, i.e., the weight matrix is $W_{10} = \begin{pmatrix} 1 & 0 \\ 0 & 0 \end{pmatrix}$ or $W_{01} = \begin{pmatrix} 0 & 0 \\ 0 & 1 \end{pmatrix}$. The green line represents the total estimation error when the two frequencies are estimated by single-parameter estimation schemes, i.e., one frequency is estimated and the other is assumed to be known each time. The true values for B, ω_1, and ω_2 are 1.2, 1, and 1.1.

5. Conclusion

In this work, we considered a simple model of a qubit in an oscillating magnetic field with multiple unknown frequencies, and studied the effect of optimization on the initial state preparation and the Hamiltonian control for the improvement of the precision limit in simultaneously estimating the two oscillation frequencies. The precision limit of estimating the frequencies is quantified by the most informative bound, which minimizes the Cramér–Rao bound over all measurement basis on the quantum system and is therefore always a tight and attainable precision bound of quantum multi-parameter estimation. Results show that both the optimizations on the initial state and the Hamiltonian control are capable of providing a higher precision limit than without any optimization, and the optimizations are implemented with the quasi-Newton method from the numerical optimization theory due to the distinctive advantage of this method compared to the steepest descent method or the Newton's method. In addition to the increase of the precision limit, it is found that the optimized scheme demonstrates better robustness in estimating the frequencies against the deviation between the approximate values of the parameters used in the control scheme and the true values of the parameters than that without any optimization. Moreover, the precisions of estimating the two frequencies simultaneously and individually are also investigated, and the result manifests the difference between the multi-parameter estimation and the single-parameter estimation.

Appendix A: Quasi-Newton method

The optimization of the Cramér–Rao bound over all possible POVM's in the most informative bound is generally difficult to be worked out by analytical method due to the complexity of the Cramér–Rao bound, so we will resort to numerical optimization methods to obtain the most informative bound in the following sections of this paper as in other literature.[7–9,35,67]

There are different approaches for numerical optimization, e.g., the steepest descent method, the Newton's method, etc. The quasi-Newton method is a development from the Newton's method.[69] The advantage of Newton's method lies in its second-order convergence speed, compared to the steepest descent method, but its disadvantage is the complexity of calculating the Hessian matrix, which involves the second-order derivatives of the optimized function with respect to different parameters. The quasi-Newton method preserves the advantage of Newton's method by constructing an approximate matrix for the Hessian matrix and also maintains a fast convergence speed as the approximate matrix only involves the first-order derivatives of the optimized function, which keeps a good balance between the convergence speed and the computational complexity.

Due to the above advantage of the quasi-Newton method, we will employ the quasi-Newton method to obtain the optimal initial state, the optimal Hamiltonian control, and optimal measurement that can minimize the most informative bound in this paper.

The procedures of the quasi-Newton algorithm for the current multi-parameter quantum metrology problem are outlined as follows:

(i) Select a set of initial values $x^{(0)}$ for the initial state, the Hamiltonian control and the final measurement, as well as an

initial approximate matrix B_0 of the Hessian matrix which is generally assumed to be the identity matrix. Let $k := 0$, $\varepsilon > 0$.

(ii) Compute the evolution of the quantum system under the given Hamiltonian, the most informative bound $F_{\mathrm{MI}}^{(k)}$ as well as the gradient of the most informative bound with respect to the parameters to be optimized, $\nabla F_{\mathrm{MI}}^{(k)}$. If $\left\|\nabla F_{\mathrm{MI}}^{(k)}\right\| \leq \varepsilon$, the algorithm terminates, yielding the solution $x^{(k)}$. The superscript (k) in $F_{\mathrm{MI}}^{(k)}$ denote that it is the most informative bound at the k-th iterative step.

(iii) Solve the system of linear equations

$$B_k d^{(k)} + \nabla F_{\mathrm{MI}}^{(k)} = 0, \tag{A1}$$

yielding the solution $d^{(k)}$.

(iv) Determine the optimal step size parameter α_k by linear search, and let

$$x^{(k+1)} = x^{(k)} + \alpha_k d^{(k)}. \tag{A2}$$

(v) If $\left\|\nabla F_{\mathrm{MI}}^{(k+1)}\right\| \leq \varepsilon$, the algorithm terminates, yielding the solution $x^{(k+1)}$ to the problem. Otherwise, one obtains B_{k+1} by

$$B_{k+1}(x^{(k+1)} - x^{(k)}) = \nabla f(x^{(k+1)}) - \nabla f(x^{(k)}). \tag{A3}$$

(vi) Let $k := k+1$, and go to step (iii).

Acknowledgement

Project supported by the National Natural Science Foundation of China (Grant No. 12075323).

References

[1] Holevo A 2011 *Probabilistic and Statistical Aspects of Quantum Theory*
[2] Helstrom C W 1969 *Journal of Statistical Physics* **1** 231
[3] Braunstein S L and Caves C M 1994 *Phys. Rev. Lett.* **72** 3439
[4] Huelga S F, Macchiavello C, Pellizzari T, Ekert A K, Plenio M B and Cirac J I 1997 *Phys. Rev. Lett.* **79** 3865
[5] Niu C and Yu S 2024 *Chin. Phys. B* **33** 20304
[6] Liu J, Lu X M, Sun Z and Wang X 2016 *J. Phys. A: Math. Theor.* **49** 115302
[7] Liu J and Yuan H 2017 *Phys. Rev. A* **96** 042114
[8] Liu J and Yuan H 2017 *Phys. Rev. A* **96** 012117
[9] Xu H, Li J, Liu L, Wang Y, Yuan H and Wang X 2019 *npj Quantum Information* **5** 1
[10] Zhou S, Zhang M, Preskill J and Jiang L 2018 *Nat. Commun.* **9** 78
[11] Zhou S and Jiang L 2020 *Phys. Rev. Res.* **2** 013235
[12] Dür W, Skotiniotis M, Fröwis F and Kraus B 2014 *Phys. Rev. Lett.* **112** 080801
[13] Kessler E M, Lovchinsky I, Sushkov A O and Lukin M D 2014 *Phys. Rev. Lett.* **112** 150802
[14] Unden T, Balasubramanian P, Louzon D, Vinkler Y, Plenio M B, Markham M, Twitchen D, Stacey A, Lovchinsky I, Sushkov A O, Lukin M D, Retzker A, Naydenov B, McGuinness L P and Jelezko F 2016 *Phys. Rev. Lett.* **116** 230502
[15] Tan K C, Omkar S and Jeong H 2019 *Phys. Rev. A* **100** 022312
[16] Mahmud K W, Tiesinga E and Johnson P R 2014 *Phys. Rev. A* **90** 041602
[17] Pang S and Jordan A N 2017 *Nat. Commun.* **8** 14695
[18] Yuan H 2016 *Phys. Rev. Lett.* **117** 160801
[19] Hou Z, Jin Y, Chen H, Tang J F, Huang C J, Yuan H, Xiang G Y, Li C F and Guo G C 2021 *Phys. Rev. Lett.* **126** 070503
[20] Wan K and Lasenby R 2022 *Phys. Rev. Res.* **4** 033092
[21] Yang J, Pang S, Chen Z, Jordan A N and del Campo A 2022 *Phys. Rev. Lett.* **128** 160505
[22] Hong H, Lu X and Kuang S 2023 *Chin. Phys. B* **32** 40603
[23] Valeri M, Polino E, Poderini D, Gianani I, Corrielli G, Crespi A, Osellame R, Spagnolo N and Sciarrino F 2020 *npj Quantum Information* **6** 92
[24] Markiewicz M, Pandit M and Laskowski W 2021 *Sci. Rep.* **11** 15669
[25] Xia B, Huang J, Li H, Wang H and Zeng G 2023 *Nat. Commun.* **14** 1021
[26] Yin P, Zhao X, Yang Y, Guo Y, Zhang W H, Li G C, Han Y J, Liu B H, Xu J S, Chiribella G, Chen G, Li C F and Guo G C 2023 *Nat. Phys.* **19** 1122
[27] Leibfried D, Barrett M D, Schaetz T, Britton J, Chiaverini J, Itano W M, Jost J D, Langer C and Wineland D J 2004 *Science* **304** 1476
[28] Eisenberg H S, Hodelin J F, Khoury G and Bouwmeester D 2005 *Phys. Rev. Lett.* **94** 090502
[29] Chen G, Zhang L, Zhang W H, Peng X X, Xu L, Liu Z D, Xu X Y, Tang J S, Sun Y N, He D Y, Xu J S, Zhou Z Q, Li C F and Guo G C 2018 *Phys. Rev. Lett.* **121** 060506
[30] Treps N, Grosse N, Bowen W P, Fabre C, Bachor H A and Lam P K 2003 *Science* **301** 940
[31] Morris P A, Aspden R S, Bell J E C, Boyd R W and Padgett M J 2015 *Nat. Commun.* **6** 5913
[32] Casacio C A, Madsen L S, Terrasson A, Waleed M, Barnscheidt K, Hage B, Taylor M A and Bowen W P 2021 *Nature* **594** 201
[33] Taylor M A, Janousek J, Daria V, Knittel J, Hage B, Bachor H A and Bowen W P 2013 *Nat. Photon.* **7** 229
[34] Hou Z, Tang J F, Chen H, Yuan H, Xiang G Y, Li C F and Guo G C 2021 *Sci. Adv.* **7** eabd2986
[35] Xiao T, Fan J and Zeng G 2022 *npj Quantum Information* **8** 2
[36] Nagata T, Okamoto R, O'Brien J L, Sasaki K and Takeuchi S 2007 *Science* **316** 726
[37] Resch K J, Pregnell K L, Prevedel R, Gilchrist A, Pryde G J, O'Brien J L and White A G 2007 *Phys. Rev. Lett.* **98** 223601
[38] Chen G, Aharon N, Sun Y N, Zhang Z H, Zhang W H, He D Y, Tang J S, Xu X Y, Kedem Y, Li C F and Guo G C 2018 *Nat. Commun.* **9** 93
[39] Cramér H 2016 *Mathematical Methods of Statistics* (PMS-9), Vol. 9 (Princeton University Press)
[40] Giovannetti V, Lloyd S and Maccone L 2011 *Nat. Photon.* **5** 222
[41] Giovannetti V, Lloyd S and Maccone L 2006 *Phys. Rev. Lett.* **96** 010401
[42] Řehaček J, Hradil Z, Stoklasa B, Paúr M, Grover J, Krzic A and Sánchez-Soto L L 2017 *Phys. Rev. A* **96** 062107
[43] Shih Y 2007 *IEEE J. Select. Top. Quantum Electron.* **13** 1016
[44] Degen C L, Reinhard F and Cappellaro P 2017 *Rev. Mod. Phys.* **89** 035002
[45] Shabani A, Mohseni M, Lloyd S, Kosut R L and Rabitz H 2011 *Phys. Rev. A* **84** 012107
[46] Cole J H, Greentree A D, Oi D K L, Schirmer S G, Wellard C J and Hollenberg L C L 2006 *Phys. Rev. A* **73** 062333
[47] Zhang J and Sarovar M 2014 *Phys. Rev. Lett.* **113** 080401
[48] Wang Y, Dong D, Qi B, Zhang J, Petersen I R and Yonezawa H 2018 *IEEE Trans. Autom. Control* **63** 1388
[49] Lu X M, Ma Z and Zhang C 2020 *Phys. Rev. A* **101** 022303
[50] Helstrom C W 1967 *Phys. Lett. A* **25** 101
[51] Yuen H and Lax M 1973 *IEEE Trans. Inform. Theory* **19** 740
[52] Belavkin V P 1976 *Theor. Math. Phys.* **26** 213
[53] Suzuki J 2019 *Entropy* **21** 703
[54] Albarelli F, Barbieri M, Genoni M G and Gianani I 2020 *Phys. Lett. A* **384** 126311
[55] Ragy S, Jarzyna M and Demkowicz-Dobrzański R 2016 *Phys. Rev. A* **94** 052108
[56] Humphreys P C, Barbieri M, Datta A and Walmsley I A 2013 *Phys. Rev. Lett.* **111** 070403
[57] Szczykulska M, Baumgratz T and Datta A 2016 *Adv. Phys.: X* **1** 621
[58] Baumgratz T and Datta A 2016 *Phys. Rev. Lett.* **116** 030801
[59] Gagatsos C N, Branford D and Datta A 2016 *Phys. Rev. A* **94** 042342
[60] Yao Y, Ge L, Xiao X, Wang X G and Sun C P 2014 *Phys. Rev. A* **90** 022327
[61] Zhang Y R and Fan H 2014 *Phys. Rev. A* **90** 043818

[62] Yao Y, Ge L, Xiao X, Wang X and Sun C P 2014 *Phys. Rev. A* **90** 062113
[63] Knott P A, Proctor T J, Hayes A J, Ralph J F, Kok P and Dunningham J A 2016 *Phys. Rev. A* **94** 062312
[64] Berry D W, Tsang M, Hall M J W and Wiseman H M 2015 *Phys. Rev. X* **5** 031018
[65] Yue J D, Zhang Y R and Fan H 2014 *Sci. Rep.* **4** 5933
[66] Yuan H and Fung C H F 2015 *Phys. Rev. Lett.* **115** 110401
[67] Xu H, Wang L, Yuan H and Wang X 2021 *Phys. Rev. A* **103** 042615
[68] Khaneja N, Reiss T, Kehlet C, Schulte-Herbrüggen T and Glaser S J 2005 *Journal of Magnetic Resonance* **172** 296
[69] William H. Press, Saul A Teukolsky, William T Vetterling and Brian P Flannery 1992 *Numerical Recipes in C: The Art of Scientific Computing*, 2nd edn. (USA: Cambridge University Press)
[70] Care C M 1983 *Phys. Bull.* **34** 395
[71] Suzuki J, Yang Y and Hayashi M 2020 *J. Phys. A: Math. Theor.* **53** 453001
[72] Suzuki J 2020 *J. Phys. A: Math. Theor.* **53** 264001